embryo cDNA library fused to the transcription activation domain of yeast GAL4 in the vector pGAD10 and isolated three independent partial clones of the *d-axin* cDNA. A larger partial *d-axin* cDNA clone (2.7 kb) was isolated by rescreening a λgt11 *Drosophila* embryo cDNA library with the smaller cDNAs, and the remaining 5′-end region was obtained by the 5′ RACE (rapid amplification of cDNA ends) technique (Clontech). Multiple independent polymerase chain reaction (PCR) products were analyzed to exclude the possibility of PCR-induced errors. Sequence comparison analysis was performed with the *blastp* program [S. F. Altschul *et al.*, *Nucleic Acids Res.* **25**, 3389 (1997)].
6. L. Zeng *et al.*, *Cell* **90**, 181 (1997).
7. J. Behrens *et al.*, *Science* **280**, 596 (1998).
8. S. Ikeda *et al.*, *EMBO J.* **17**, 1371 (1998); C. Sakanaka, J. B. Weiss, L. T. Williams, *Proc. Natl. Acad. Sci. U.S.A.* **95**, 3020 (1998); H. Yamamoto *et al.*, *Mol. Cell. Biol.* **18**, 2867 (1998); S. Kishida *et al.*, *J. Biol. Chem.* **273**, 10823 (1998); K. Itoh, V. E. Krupnik, S. Y. Sokol, *Curr. Biol.* **8**, 591 (1998); M. J. Hart, R. de los Santos, I. N. Albert, B. Rubinfeld, P. Polakis, *ibid.*, p. 573.
9. T. Nakamura *et al.*, *Genes Cells* **3**, 395 (1998).
10. Full-length D-Axin and the Armadillo repeat domain of Arm were labeled with ^{35}S-methionine with the coupled transcription-translation TNT system (Promega). GST and GST-fusion proteins (2 μg) immobilized to glutathione-Sepharose beads were mixed with in vitro–translated proteins in binding buffer [20 mM tris-HCl (pH 8.0), 140 mM NaCl, 1 mM EDTA, 1 mM dithiothreitol, 10% glycerol, 1% Triton X-100, and 10 μg/ml each of aprotinin, leupeptin, and pepstatin) for 1 hour at 4°C. After washing five times with binding buffer, bound proteins were fractionated by SDS–polyacrylamide gel electrophoresis (PAGE) followed by autoradiography.
11. F. Hamada *et al.*, unpublished data.
12. S. Hayashi *et al.*, *Proc. Natl. Acad. Sci. U.S.A.* **94**, 242 (1997).
13. Using in situ hybridization to polytene chromosomes, we mapped the *d-axin* gene to 99D in the third chromosome. The genomic P1 clone DS00026 from the Berkeley *Drosophila* Genome Project contained the genomic region corresponding to the *d-axin* cDNA. The genomic organization of the *d-axin* locus and the intron-exon structure were determined by Southern (DNA) blot analysis and subsequent sequencing across the exon-intron boundaries.
14. A *Drosophila* strain containing the P-element–induced lethal line *l(3)S044230* was obtained from the European *Drosophila* P-element–induced lethal stock center (Szeged Center, Hungary). The precise point of P-element insertion was determined by genomic sequencing. Association of the observed lethal phenotype with the P-element insertion was confirmed by mobilization of the P-element with a Ki, p^{p}, Δ2-3 strain [H. M. Robertson *et al.*, *Genetics* **118**, 461 (1988)].
15. The GAL4/UAS system was used for overexpression of *d-axin* [A. H. Brand and N. Perrimon, *Development* **118**, 401 (1993)]. The entire *d-axin* open reading frames of various constructs were subcloned into the pUAST vector and introduced into the *w* germ line by the standard P-element transformation method. These UAS-*d-axin* lines were crossed with several GAL4 drivers [Y. Shiga, M. Tanaka-Matakatsu, S. Hayashi, *Dev. Growth Differ.* **38**, 99 (1996); E. J. Rulifson, C. A. Micchelli, J. D. Axelrod, N. Perrimon, S. S. Blair, *Nature* **384**, 72 (1996)].
16. Germ-line clones of *d-axin* were generated by use of the FLP-DFS technique [T. B. Chou and N. Perrimon, *Genetics* **144**, 1673 (1996)]. All embryos derived from homozygous *d-axin* germ-line clones die during embryonic development. The TM3 *gfp* chromosome was used to determine the zygotic genotype of embryos. Cuticles were prepared and mounted in Hoyer's medium [J. van der Meer, *Drosophila Inf. Serv.* **52**, 160 (1977)], viewed, and photographed under dark field.
17. E. Siegfried, E. L. Wilder, N. Perrimon, *Nature* **367**, 76 (1994); M. Zecca, K. Basler, G. Struhl, *Cell* **87**, 833 (1996).
18. K. Irvine and T. F. Vogt, *Curr. Opin. Cell. Biol.* **9**, 867 (1997).
19. *d-axin* mutant clones were generated by use of the FLP-FRT technique [T. Xu and G. M. Rubin, *Development* **117**, 1223 (1993)]. Genotypes for generated clones are *y w hsp-flp.1/w* or *Y; FRT82 d-axin^{S044230}/FRT82 hsp-CD2, y^{+}* for adults and *y w hsp-flp.1/w* or *Y; FRT82 d-axin^{S044230}/FRT82 hsp70-myc-gfp, w^{+}* for imaginal discs [J. Jiang and G. Struhl, *Nature* **391**, 493 (1998)]. Mutant phenotypes were induced in the mid–second instar larval stage by heat shock at 37°C for 30 min. For the induction of the *hsp70-myc-gfp* gene, wandering larvae were heat shocked at 37°C for 60 min and then processed for immunostaining after a 60-min recovery period at 25°C. The mutant clones can be recognized by the *y* marker in adults and by the absence of GFP expression in the imaginal discs, respectively.
20. W. J. Brook and S. M. Cohen, *Science* **273**, 1373 (1996); J. Jiang and G. Struhl, *Cell* **86**, 401 (1996); A. Penton and F. M. Hoffmann, *Nature* **382**, 162 (1996).
21. A. D. Shirras and J. P. Couso, *Dev. Biol.* **175**, 24 (1996).
22. C. J. Neumann and S. M. Cohen, *Development* **124**, 871 (1997); K. M. Cadigan, M. P. Fish, E. J. Rulifson, R. Nusse, *Cell* **93**, 767 (1998).
23. Wing imaginal discs from third instar larvae were dissected, fixed, and stained with mouse antibodies to Arm (anti-Arm, N2-7A1) [M. Peifer, D. Sweeton, M. Casey, E. Wieschaus, *Development* **120**, 369 (1994)] or anti-Dll [G. Vachon *et al.*, *Cell* **71**, 437 (1992)]. These antibodies were detected with rhodamine-conjugated goat anti-mouse immunoglobulin G (Jackson Immunochemicals). Confocal fluorescent images were obtained with a Zeiss LSM510 microscope.
24. We thank J. Jiang, G. Struhl, the Bloomington Stock Center, and the European Drosophila P-element–induced Lethal Stock Center (Szeged Center) for fly stocks; S. Yanagawa, S. Cohen, and E. Wieschaus for plasmids and antibodies; the Berkeley Drosophila Genome Project and E. Nitasaka for genomic P1 clones; A. Ogai, Y. Katoh, N. Kakinuma, T. Shikina, T. Wada, A. Furui, and M. Ichikawa for technical assistance; and S. Higashijima, E. Shishido, T. Tabata, and K. W. Cho for helpful discussions. Supported by grants from the Ministry of Education, Science, and Culture of Japan and the National Institute for Basic Biology Cooperative Research Program.

6 October 1998; accepted 9 February 1999

Truncated RanGAP Encoded by the *Segregation Distorter* Locus of *Drosophila*

Cynthia Merrill, Leyla Bayraktaroglu,* Ayumi Kusano, Barry Ganetzky†

***Segregation Distorter* (*SD*) in *Drosophila melanogaster* is a naturally occurring meiotic drive system in which the *SD* chromosome is transmitted from *SD/SD^{+}* males in vast excess over its homolog owing to the induced dysfunction of *SD^{+}*-bearing spermatids. The *Sd* locus is the key distorting gene responsible for this phenotype. A genomic fragment from the *Sd* region conferred full distorting activity when introduced into the appropriate genetic background by germline transformation. The only functional product encoded by this fragment is a truncated version of the RanGAP nuclear transport protein. These results demonstrate that this mutant RanGAP is the functional *Sd* product.**

Examples of meiotic drive, in which a particular allele or chromosome of a heterozygous pair is preferentially transmitted to the offspring, have been described in natural populations of fungi, plants, insects, and mammals (*1*). This violation of the fundamental principle of Mendelian genetics can subvert the evolutionary process, which is contingent on the unbiased exposure of competing genes to selective forces. The molecular mechanisms of meiotic drive have remained elusive.

One of the best characterized meiotic drive systems is *Segregation Distorter* (*SD*) in *Drosophila melanogaster* (*2*). *SD* chromosomes are transmitted from *SD/SD^{+}* males to more than 95% of the progeny; transmission from females is normal. *Sd*, a dominant gain-of-function mutation, is the primary gene on *SD* chromosomes required for distortion. Strong distortion also requires several linked modifier loci, including *Enhancer* [*E(SD)*], *Modifier* [*M(SD)*], and *Stabilizer* [*St(SD)*] (*2–4*). The target of distortion is the *Responder* (*Rsp*) locus, which consists of an array of repeated satellite sequences whose copy number is correlated with sensitivity (*4, 5*). Chromosomes carrying *Rsp^{s}* (sensitive) or *Rsp^{ss}* (supersensitive) loci are subject to distortion, whereas *SD* chromosomes, which carry *Rsp^{i}* (insensitive), are resistant. Distortion ultimately involves sperm dysfunction, first visibly apparent as failed chromatin condensation in half of the developing spermatids (*6*).

The *Sd* locus was isolated by positional cloning and found to be associated with a tandem duplication that replaces the wild-type (*Sd^{+}*) 6.5-kb Eco RI fragment with an 11.5-kb Eco RI fragment (*7*). When introduced into appropriate genetic backgrounds by germline transformation, the 11.5-kb fragment confers full distortion, which indicates that *Sd* activity is contained entirely within this fragment (*8*). Transformants that have

Laboratory of Genetics, 445 Henry Mall, University of Wisconsin, Madison, WI 53706, USA.

*Present address: Department of Molecular and Cellular Biology, Harvard University, 16 Divinity Avenue, Cambridge, MA 02138, USA.

†To whom correspondence should be addressed. E-mail: ganetzky@facstaff.wisc.edu

lost either half of the duplication fail to cause distortion, demonstrating that *Sd* activity requires juxtaposition of particular sequences in both halves of the duplication.

To identify the particular gene or genes within the duplication that are responsible for distortion, we sequenced the 6.5-kb Sd^+ and 11.5-kb *Sd* genomic clones as well as cDNAs derived from these chromosome segments. Two nested transcription units were identified in Sd^+, both of which are represented twice in the duplication (Fig. 1, A and B). One of these genes (*dHS2ST*) encoded the *Drosophila* homolog of mammalian heparan-sulfate 2-sulfotransferase (*9*). The other, *dRanGAP*, was identified as the *Drosophila* homolog of mammalian *RanGAP1*, the guanosine triphosphatase (GTPase) activator for the Ras-related nuclear regulatory protein Ran (*10, 11*).

The organization of the two transcription units in the proximal half of the *Sd* duplication is essentially the same as in Sd^+ (Fig. 1, A and B). Although the proximal *dHS2ST* transcript in some *SD* lines contained a premature stop codon, resulting in truncation of 46 amino acids, other strongly distorting lines lacked this single base polymorphism. The proximal *dRanGAP* transcript is identical with the wild type except for a 9–base pair (bp) deletion near the 3′ end. Because this deletion occurs outside the 11.5-kb fragment, this polymorphism is also unlikely to be responsible for the *Sd* phenotype.

The *dHS2ST* transcript in the distal half of the duplication encoded a wild-type protein. A cDNA representing a previously identified *SD*-specific 4.2-kb transcript (*8, 9*) initiated in the proximal half of the duplication and read through the distal copy of the *dHS2ST* gene, resulting in an aberrant mRNA that contained a wild-type *dHS2ST* coding region preceded by a long untranslated leader (Fig. 1B).

The remaining distal transcript encoded a mutant version of dRanGAP whose COOH-terminal portion differed from that of the wild type beginning at the duplication junction (Fig. 1B). Analysis of *SD* cDNAs (*10*) indicated that the distal *dRanGAP* transcript extended about 300 to 400 bp beyond the junction into the proximal half of the duplication. The juxtaposition of sequences at the junction site introduced an in-frame stop codon immediately adjacent to this site. The resulting *dRanGAP* mRNA encoded a truncated polypeptide missing 234 amino acids at the COOH-terminus (*12*). Because this truncated dRanGAP was the only substantially altered protein encoded by the 11.5-kb fragment, and because its generation required the fusion of sequences from both halves of the duplication, it was the best candidate for the *Sd* gene product.

To be capable of causing distortion, the postulated truncated dRanGAP must be stable and expressed in testes. The *dRanGAP* cDNA sequences predict proteins of 66 kD encoded both by Sd^+ and by the proximal half of the *Sd* duplication, as well as an *Sd*-specific 40-kD protein encoded by the distal half of the *Sd* duplication. Affinity-purified antiserum (*13*) detected the expected 66-kD protein in males of all genotypes on protein immunoblots of protein extracts from testes (Fig. 2, lanes 1 through 7). The 40-kD protein was detected in all native *SD* lines examined but not in the wild type (Fig. 2, lanes 1 and 2) (*14, 15*). Furthermore, three independent germline transformants for the 11.5-kb duplication that showed strong distorting activity expressed the truncated protein (Fig. 2, lanes 3 through 5), whereas another transformant that spontaneously lost part of the duplication and failed to distort did not express this protein (Fig. 2, lane 6). Thus, expression of

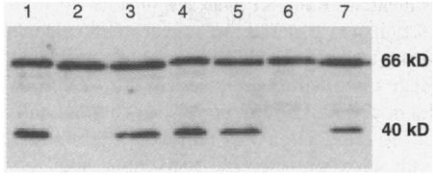

Fig. 2. Protein immunoblot of testes proteins probed with *Drosophila* antibodies to RanGAP. Three pair of testes were dissected from newly eclosed flies, boiled in SDS sample buffer, and run on a 15% polyacrylamide gel. The proteins were transferred to nitrocellulose and probed with a polyclonal antiserum (1:500) raised against the amino-terminal region of wild-type dRanGAP. Horseradish peroxidase (HRP)–conjugated goat anti-rabbit secondary antibodies (Bio-Rad) (1:3000) were detected by chemiluminescence (Amersham). Lane 1, *SD-Mad*; lane 2, Canton-S (wild type); lanes 3 through 5, three independently generated transgenic lines containing the 11.5-kb *Sd* duplication (*8*). These three transformant lines show high levels of distortion. Lane 6, a transgenic line transformed originally with the 11.5-kb *Sd* duplication that has undergone spontaneous loss of a significant portion of the duplication. No distortion is observed in this line. Lane 7, transgenic flies containing the P[(w^+*Sd*)12A] transformation construct that specifically encodes the truncated form of dRanGAP. This transgenic line shows high levels of distortion.

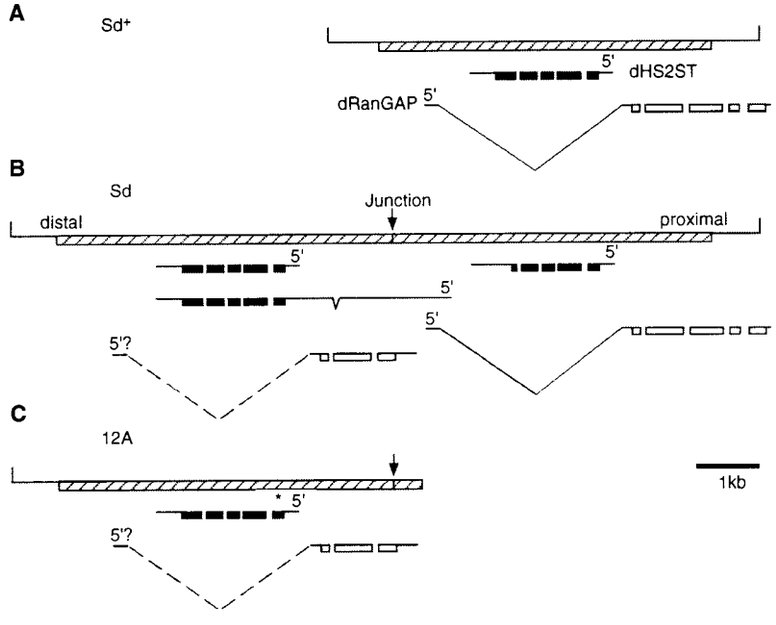

Fig. 1. Organization of *dHS2ST* and *dRanGAP* transcription units in SD^+ and *SD* genomic DNA. The upper line in each panel represents the genomic clones. The wild-type genomic sequence that is tandemly duplicated in *SD* is represented by the hatched bar. The alignment of cDNAs with the genomic sequence is indicated underneath the genomic fragment. Exons containing translated sequences are represented by boxes. Solid boxes represent *dHS2ST* exons and open boxes represent *dRanGAP* exons. A space between boxes indicates the presence of an intron. Introns in noncoding sequences are indicated by a V-shaped line. (**A**) Two cDNAs transcribed from opposite strands were identified in wild-type flies. The *dHS2ST* cDNA is entirely contained within a large (2.7-kb) intron at the 5′ end of *dRanGAP*. (**B**) The junction of the tandem duplication is marked. Each half of the duplication contains both *dHS2ST* and *dRanGAP* transcription units. The distally encoded dRanGAP polypeptide is truncated at the junction site. The 5′ end of the distal *dRanGAP* transcription unit is drawn so that it corresponds with that of the proximal *dRanGAP* transcript. However, cDNAs for this transcript are incomplete at the 5′ end, so the exact starting point is unknown. This uncertainty is indicated by the broken line representing the presumptive intron and the question mark at the 5′ end of the transcript. An aberrantly large *dHS2ST* transcript that initiates ectopically in the proximal part of the duplication and results in the production of a long 5′ untranslated leader is shown. (**C**) The 12A genomic transformation construct includes the entire distal half of the *Sd* duplication plus approximately 500 bp from the right half of the duplication. Two in-frame stop codons (asterisk) were introduced into the *dHS2ST* coding sequence to eliminate expression of this protein from the 12A transformation construct.

Table 1. Segregation distortion caused by the 12A construct expressing a truncated dRanGAP protein. The second chromosome genotype of the tested males, which includes the indicated components of the *SD* system, is shown in columns 2 and 3. At least 10 males of the indicated genotypes, either lacking (column 4) or carrying (column 5) the 12A construct inserted on the *TM3* third chromosome were individually crossed to *cn bw* females, and the progeny were scored for *cn* or *cn bw* eye color markers. *lt* and *pk* are eye color and bristle markers, respectively. The data (mean ± SD) are presented as the relative proportion of the total progeny that inherited the Rsp^{i} homolog from the tested males. The total number of offspring (*n*) counted for each cross is indicated beneath the segregation ratios. The data have been corrected for small intrinsic viability differences associated with the segregating homologs as described in (*8*).

Row	Genotype	*SD* components present	12A absent	12A present
1	Rsp^{i16} *cn bw*/Rsp^{ss} *lt*/*pk cn*	Rsp^{i}/Rsp^{ss}	0.490 ± 0.056 (*n* = 2063)	0.568 ± 0.064 (*n* = 1896)
2	*SD-5*^{Rev7}/Rsp^{ss} *lt pk cn*	E(SD) Rsp^{i} M(SD) St(SD)/Rsp^{ss}	0.509 ± 0.085 (*n* = 910)	0.980 ± 0.037 (*n* = 929)
3	*SD-5*^{Rev7}/Rsp^{i} *cn bw*	E(SD) Rsp^{i} M(SD) St(SD)/Rsp^{i}	0.494 ± 0.055 (*n* = 791)	0.516 ± 0.070 (*n* = 2371)
4	*SD-Mad*^{Rev77}/Rsp^{ss} *lt pk cn*	E(SD) Rsp^{i} M(SD) St(SD)/Rsp^{ss}	0.507 ± 0.058 (*n* = 987)	0.845 ± 0.079 (*n* = 2973)
5	*SD-Mad*^{Rev77}/Rsp^{i} *cn bw*	E(SD) Rsp^{i} M(SD) St(SD)/Rsp^{i}	0.487 ± 0.062 (*n* = 2263)	0.537 ± 0.083 (*n* = 1909)
6	*SD-5*^{Rev16}/Rsp^{ss} *lt pk cn*	Su(SD) Sd E(SD) Rsp^{i} M(SD) St(SD)/Rsp^{ss}	0.494 ± 0.045 (*n* = 2392)	0.472 ± 0.061 (*n* = 943)

an *Sd*-specific truncated dRanGAP correlated with distorting activity.

To test directly whether expression of the truncated dRanGAP was responsible for distortion, we generated a transformation construct capable of expressing only this protein. Beginning with the intact 11.5-kb Eco RI fragment, all but 562 bp of the proximal half of the duplication was removed to eliminate both proximal-specific transcripts and the 4.2-kb version of the distal *dHS2ST* transcript (Fig. 1C). The coding potential of the remaining distal-specific *dHS2ST* transcript was abolished by introducing two in-frame stop codons. We used this modified genomic construct to generate a germline transformant, P[($w^{+}Sd$)12A]. This construct directs the production of the *Sd*-specific 40-kD dRanGAP protein although its level of expression appeared somewhat reduced (Fig. 2, lane 7) (*15*).

We introduced P[($w^{+}Sd$)12A] into different genetic backgrounds where the other components of the *SD* system were varied and tested its ability to cause distortion. The resulting segregation ratios are shown in Table 1. Distortion is indicated by the excess transmission of the Rsp^{i} chromosome relative to the Rsp^{ss} homolog. In the absence of any upwards modifiers of *Sd*, P[($w^{+}Sd$)12A] caused only a low level of distortion (Table 1, row 1). This result corresponds with results obtained for the intact 11.5-kb duplication as well as for native *Sd* in the absence of other drive elements (*8*). To introduce the full constellation of modifier loci, we used derivatives of two different *SD* chromosomes, *SD-5*^{Rev7} and *SD-Mad*^{Rev77}, from which the *Sd* locus had been deleted, leaving the other drive elements intact (*4, 16*). These reverted *SD* chromosomes have completely lost the ability to distort (Table 1, rows 2 and 4). However, when P[($w^{+}Sd$)12A] was introduced into these backgrounds, strong distortion of the Rsp^{ss} chromosome was observed in both cases (Table 1, rows 2 and 4). The strength of distortion caused by P[($w^{+}Sd$)12A] varied with the insertion site, as full distortion in both backgrounds was observed when the insert was remobilized to new locations (*15*). The complete distortion caused by P[($w^{+}Sd$)12A] in the appropriate background establishes its functional equivalence to *Sd*. To demonstrate that this distortion depended exclusively on the action of the *SD* system, comparable crosses were carried out in which both homologs carried a Rsp^{i} allele. As expected, no distortion was observed in these backgrounds whether or not P[($w^{+}Sd$)12A] was present (Table 1, rows 3 and 5). Furthermore, distortion by P[($w^{+}Sd$)12A] was eliminated in the presence of *SD-5*^{Rev16}, a strong suppressor of distortion (*4*) (Table 1, row 6). Thus, P[($w^{+}Sd$)12A] reproduces the behavior of a native *Sd* in every respect. Therefore, we conclude that the truncated dRanGAP is the functional *Sd* product (*17*).

Much recent work in yeast and mammalian cells has shown that nucleocytoplasmic transport is dependent on the small nuclear GTPase Ran (*18*). Genetic and biochemical data demonstrate that regulators such as the guanine nucleotide exchange factor (RanGEF) and the GTPase-activating protein RanGAP1, which cycle Ran between its GTP- and GDP-bound forms, are also critical (*18*). Ran and its cofactors have also been implicated in other functions, including cell cycle progression, RNA synthesis and processing, and maintenance of nuclear structure, but it remains unclear whether the effects on these processes are direct or secondary to effects on nuclear transport (*18*). In either case, the central role played by Ran and its regulators in coordinating key events of nuclear function place them in an ideal position to be subverted by a meiotic drive system. For example, *Sd* may preferentially impair nuclear transport in Rsp^{s}-bearing spermatids at a key stage in their development. The asymmetric effect on Rsp^{s}- but not Rsp^{i}-bearing spermatids could result either from biased distribution of the mutant dRanGAP to the affected spermatids or from enhanced sensitivity of Rsp^{s}-bearing spermatids to impaired nuclear transport.

References and Notes

1. T. W. Lyttle, *Annu. Rev. Genet.* **25**, 511 (1991).
2. R. G. Temin *et al.*, *Am. Nat.* **137**, 287 (1991); T. W. Lyttle, *Trends Genet.* **9**, 205 (1993).
3. L. Sandler and Y. Hiraizumi, *Genetics* **45**, 1269 (1960); D. L. Hartl, *ibid.* **76**, 477 (1974); Y. Hiraizumi, D. W. Martin, I. A. Eckstrand, *ibid.* **95**, 693 (1980).
4. B. Ganetzky, *ibid.* **86**, 321 (1977).
5. C.-I. Wu, T. W. Lyttle, M.-L. Wu, G.-F. Lin, *Cell* **54**, 179 (1988); S. Pimpinelli and P. Dimitri, *Genetics* **121**, 765 (1989).
6. K. T. Tokuyasu, W. J. Peacock, R. W. Hardy, *J. Ultrastruct. Res.* **58**, 96 (1977).
7. P. Powers and B. Ganetzky, *Genetics* **129**, 133 (1991).
8. J. McLean, C. Merrill, P. Powers, B. Ganetzky, *ibid.* **137**, 201 (1994).
9. M. Kobayashi, H. Habuchi, M. Yoneda, O. Habuchi, K. Kimata, *J. Biol. Chem.* **272**, 13980 (1997); S. Bullock, J. M. Fletcher, R. S. P. Beddington, V. A. Wilson, *Genes Dev.* **12**, 1894 (1998).
10. We used the 6.5-kb wild-type genomic fragment to screen libraries for wild-type and *Sd* cDNAs. Wild-type *dHS2ST* and *dRanGAP* cDNAs were isolated from a testes cDNA library provided by T. Hazelrigg. *Sd* cDNAs were isolated from an *Sd-Mad* male cDNA library that we constructed (Stratagene). We also constructed both wild-type and *Sd-Mad* Marathon cDNA libraries (Clontech) to extend incomplete cDNAs by polymerase chain reaction (PCR). Reverse transcription PCR was used to verify cDNA structure. cDNAs were mapped onto genomic DNA by direct sequence comparison.
11. Sequence alignments prepared with software (Wisconsin Package Version 9.0) from the Genetics Computer Group (Madison, WI) show that the wild-type dRanGAP polypeptide shares 34 and 36% amino acid identity with the *Saccharomyces cerevisiae* and mouse counterparts, respectively. The identities with the mouse protein are distributed throughout the entire sequence of 596 amino acids but are highest in the first 400 amino acids, with 40% identity and an additional 20% amino acid similarity. The top five matches identified by BLAST searches [S. F. Altschul *et al.*, *Nucleic Acids Res.* **25**, 3389 (1997)] of protein databases with the *Drosophila* sequence are RanGAP proteins from *Xenopus*, mouse, human, sea urchin, and nematode. The probabilities that the observed degree of similarity with these proteins occurs by chance range from 1.6e − 57 to 9.6e − 102.
12. Although the truncation of 234 amino acids from the distal version of dRanGAP is the most dramatic departure from the wild type protein, there are additional polymorphisms: an M-to-I substitution at ami-

no acid position 9 in all *SD* strains examined, and a C-to-Y substitution at position 146 in only some *SD* strains. In addition, because the mutant cDNA is incomplete at the 5′ end, we have been unable to confirm that the distal dRanGAP transcript initiates at the equivalent point as the wild-type and proximal dRanGAP transcripts. If there is a difference here, it should affect only the 5′ untranslated leader and not the coding sequence.

13. A genomic fragment encoding amino acids 1 through 251 of the wild-type dRanGAP protein was cloned into the pQE30 expression vector (Qiagen) and expressed in *Escherichia coli*. The gel-purified polypeptide was injected into a rabbit, and subsequent bleeds were examined by protein immunoblot analysis for the ability to identify the wild-type and mutant dRanGAP proteins in *Drosophila* testes. The expressed protein was bound to nitrocellulose strips and incubated with crude antiserum to affinity purify the antibodies to RanGAP.
14. Ten independently isolated *SD* lines from the United States (*SD-MAD*, *SD-5*, *SD-72*, and *SD-Weymouth*), Italy (*SD-Roma*, *SD-Oviedo*, and *SD-VO17*), Spain (*SD-Los Arenos*), Japan (*SD-NH2*), and Australia (*SD-Armindale*) were examined by protein immunoblot analysis and found to express both the 66-kD and 40-kD proteins. Both proteins were present at consistent levels in testes, whole flies, carcasses (minus testes or ovaries), heads, larvae, and pupae. Because no somatic phenotypes are seen in *SD* heterozygotes or homozygotes, it is likely that some step in spermatogenesis, such as the high degree of chromatin compaction that takes place, is particularly sensitive to perturbations caused by expression of the truncated dRanGAP.
15. The apparent reduction in dRanGAP protein expression in the P[(w^+Sd)12A] transformant is likely due to the particular location of the insert on the *TM3* chromosome, because both increased and decreased levels of dRanGAP expression are observed when P[(w^+Sd)12A] is remobilized to new insertion sites (C. Merrill and B. Ganetzky, unpublished results).
16. J. Brittnacher and B. Ganetzky, *Genetics* **103**, 659 (1983).
17. Although how the truncated dRanGAP is functionally altered remains unknown, it is worth noting that the truncation eliminates the lysine residue at position 533, which is the presumed target site for covalent linkage to the small ubiquitin-related modifier SUMO-1 [S. Saitoh, R. T. Pu, M. Dasso, *Trends Biochem. Sci.* **22**, 374 (1997); R. Mahajan, L. Gerace, F. Melchior, *J. Cell Biol.* **140**, 259 (1998)]. Because this modification is essential for targeting dRanGAP to nuclear pore structures, subcellular mislocalization of the truncated dRanGAP is one potential consequence.
18. M. S. Moore and G. Blobel, *Trends Biochem. Sci.* **19**, 211 (1994); D. Gorlich and I. W. Mattaj, *Science* **271**, 1513 (1996); M. G. Rush, G. Drivas, P. D'Eustachio, *Bioessays* **18**, 103 (1996); E. Nigg, *Nature* **386**, 779 (1997); M. Dasso and R. T. Pu, *Am. J. Hum. Genet.* **63**, 311 (1998).
19. We thank R. Kreber and M. Schultz for technical assistance; M. Ashburner, A. Carpenter, T. Littleton, and R. Temin for helpful comments on the manuscript; and R. Temin for insightful discussion during the course of this work. Supported by NSF grant DMB-9014779 to B.G. This is paper number 3530 from the Laboratory of Genetics.

24 November 1998; accepted 5 February 1999

Linear Differentiation of Cytotoxic Effectors into Memory T Lymphocytes

Joseph T. Opferman,[1] Bertram T. Ober,[2] Philip G. Ashton-Rickardt[1,2,3]*

A central question in immunology is the origin of long-lived T cell memory that confers protection against recurrent infection. The differentiation of naïve T cell receptor transgenic CD8$^+$ cells into effector cytotoxic T lymphocytes (CTLs) and memory CD8$^+$ cells was studied. Memory CD8$^+$ cells that were generated after strong antigenic stimulation were the progeny of cytotoxic effectors and retained antigen-specific cytolytic activity 10 weeks after adoptive transfer to antigen-free recipient mice. Thus, potential vaccines based on CTL memory will require the differentiation of naïve cells into post-effector memory T cells.

The engagement of T cell receptors (TCRs) on CD8$^+$ T cells by antigen peptide–class I major histocompatibility complexes (pMHC) on the surface of cells leads to the proliferation and differentiation into CTLs, which lyse cells presenting antigen pMHC (*1*). After the effector phase, a period of death ensues during which activated T cells undergo apoptosis, known as activation-induced cell death (AICD) (*2*). The third phase of the T cell response is characterized by the appearance of memory cells that persist for many years. Accelerated T cell responses seen upon reexposure to antigen are due to increases in the frequency of antigen-specific T cells and to qualitative changes in memory cells that allow them to respond to antigen more efficiently than naïve cells (antigen hyperreactivity). However, the precise lineage by which naïve CD8$^+$ lymphocytes differentiate into memory cells is unclear. There are two models for the development of memory CD8$^+$ cells. The linear differentiation model predicts that memory T cells are the progeny of CTLs that escape AICD. Conversely, weak antigenic stimulation could result in memory T cells that are derived from a precursor that precedes CTLs and so differentiate through a lineage parallel to effectors (decreasing potential model) (*3*).

To address the issue of CD8$^+$ cell memory differentiation, we analyzed the development of transgenic memory CD8$^+$ cells that express a H-2D^b–restricted TCR (B6.2.16) specific for a male antigen (H-Y) (*4*). Activation of B6.2.16 CD8$^+$ cells with male cells (*5*) or H-Y peptide (*6*) gives rise to long-lived anti–H-Y memory CD8$^+$ cells that persist in the absence of antigen. In the absence of markers that distinguish between effector and memory CD8$^+$ cells, we followed the differentiation of naïve CD8$^+$ cells into effector and memory-precursor cells in vitro by "counting" the number of cell divisions. B6.2.16 CD8$^+$ cells were labeled with the vital dye carboxyfluorescein diacetate succinimidyl ester (CFSE), then incubated with H-Y peptide (*7*). The proliferation of B6.2.16 CD8$^+$ cells was controlled by using various doses of H-Y peptide for 4 days of culture, and cell division was monitored by measuring 50% decreases in CFSE fluorescence (Fig. 1A). Staining of cells with the TCR-clonotypic monoclonal antibody (mAb) T3.70 (*8*) revealed that all of the divided CD8$^+$ cells in culture were B6.2.16 TCR-positive (*9*). Low doses of antigen resulted in little cell division and little detectable anti–H-Y cytolytic activity (0.1 nM H-Y peptide: <5% specific lysis). At 100 nM H-Y peptide we observed substantial cell division and a high degree of cytolytic activity (>50% specific lysis), demonstrating that antigen dose can control the differentiation of anti–H-Y CTLs (*10*).

At a fixed antigen concentration (100 nM) over 4 days in culture, B6.2.16 CD8$^+$ cells proliferated over the first five cell divisions (generation 1, 2×10^4 cells; generation 5, 29×10^4 cells) then decreased (generation 9, 6×10^4 cells) due to AICD (Fig. 1B). We observed an increase in anti–H-Y cytolytic activity with each generation (Fig. 1C). The cytolytic activity of CD8$^+$ cells remained constant until generation 7, after which it diminished, presumably because of AICD. The onset and maintenance of cytolytic activity over the course of cell division correlated with accumulation of cytoplasmic perforin, a molecule required for efficient target cell lysis by CTLs (*11*) (Fig. 1D), and by five divisions every CD8$^+$ cell was positive for intracellular perforin (Fig. 1E) (*12*). Because every B6.2.16 CD8$^+$ cell had cytolytic machinery after five cell divisions, all cells had differentiated into effectors.

To examine the effect of antigen dose on memory cell differentiation we quantitated the number of memory cells generated from B6.2.16 CD8$^+$ cells that had been cultured with various doses (Figs. 1A and 2A). Equal numbers of naïve and activated CFSE-labeled

[1]Committee on Immunology, [2]Department of Pathology, [3]Committee on Developmental Biology, The University of Chicago, Gwen Knapp Center for Lupus and Immunology Research, Chicago, IL 60637, USA.

*To whom correspondence should be addressed. E-mail: pashton@midway.uchicago.edu